

Development of Biomimetic 3D Bioprinted Scaffolds for Osteochondral Regeneration

Benjamin Holmes¹, Jiaoyan Li¹, James D. Lee¹ and Lijie Grace Zhang^{1,2*}

1. Department of Mechanical and Aerospace Engineering, and 2. Department of Medicine, The George Washington University, Washington, DC 20052.

Introduction

Articular joint repair and regeneration continue to be largely intractable due to the poor regenerative properties of this tissue. Consequently, once injured, cartilage is much more difficult to self-heal. Further, once a cartilage lesion becomes deep enough, it continues to wear into the bone, causing a full osteochondral injury. These types of defects are even harder to treat because they encompass two different types of tissue, and require special mechanical and hierarchical tissue structure considerations. Although traditional methods such as autografts and allografts have been clinically employed to treat various osteochondral lesions, there still exist many shortcomings associated with these therapies including insufficient donor tissue, donor site morbidity, infection and transmission of disease. The objective of this project is to create a novel biologically inspired 3D tissue engineered construct via a 3D bioprinting, and to employ biomimetic coatings (such as multi walled carbon nanotubes (MWCNTs) and acetylated collagen) for osteochondral regeneration. Our osteochondral scaffold has novel "key" structural support elements which aims to create a strong cartilage-bone integration for improved osteochondral tissue regeneration.

Materials and Methods

Scaffolds designed to mimic the bi-phasic structure of the osteochondral region using the Rhinoceros 3D modeling package. Six experimental groups were designed: (1) homogenous cross-hatched structures; (2) bi-phasic structures consisting of a cross hatched pattern and an intersecting rings structures; and (3) biomimetic bi-phasic structures with key features; each of the structure with large and small pore features. Models were printed on a PrinterBot 3D printing system (Figure 1). Two sample groups were also coated with acetylated collagen and poly-L-lysine coated multi walled carbon nanotubes to create biomimetic nanostructure and improve their cytocompatibility properties.

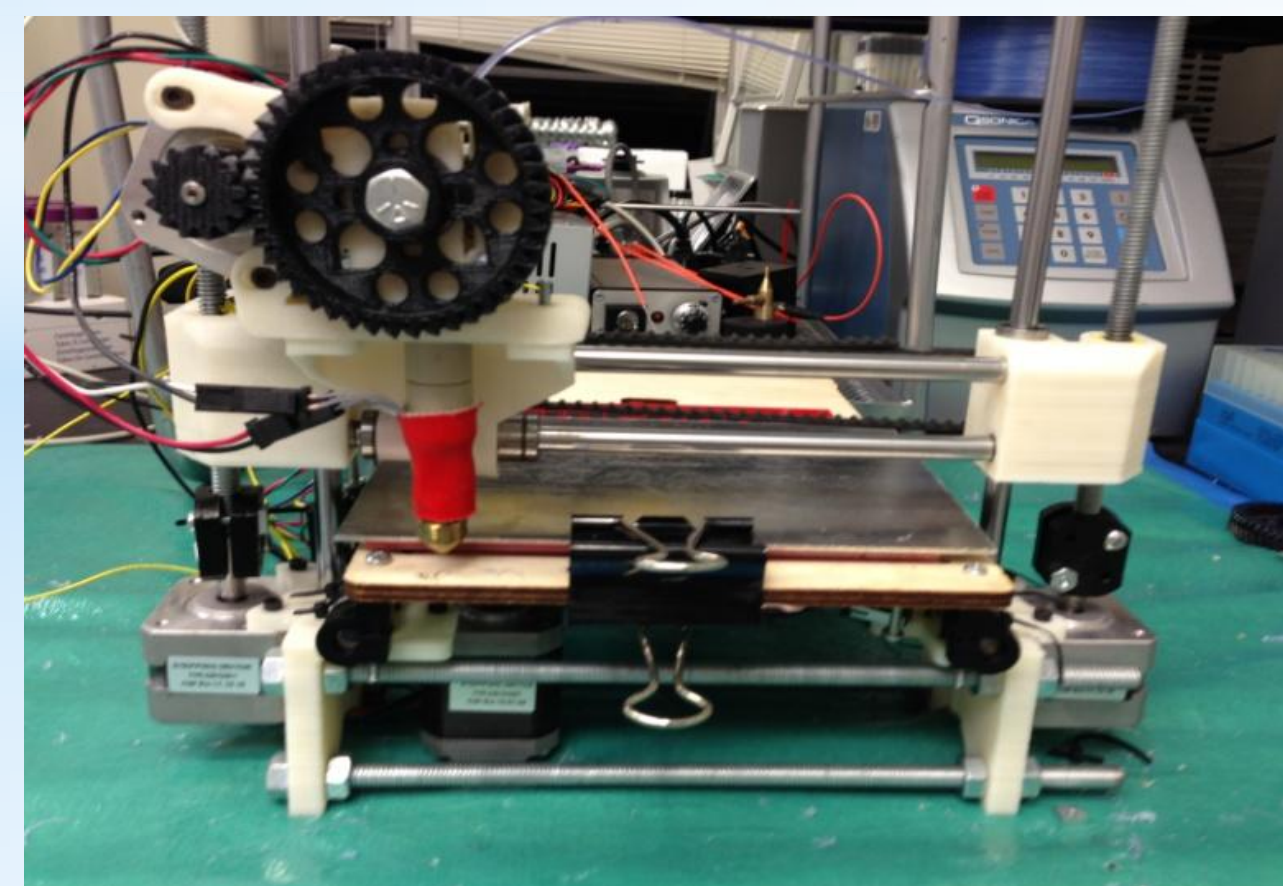


Figure 1. The lab's 3D printing setup

Scaffolds were evaluated for compressive and shear strength via a uniaxial mechanical tester. Scaffolds were also evaluated for human bone marrow mesenchymal stem cell (MSC) proliferation and 2 weeks chondrogenic differentiation *in vitro*. SEM images were taken of the surface morphology of all scaffolds.

Results

3D printing osteochondral scaffold design (I)

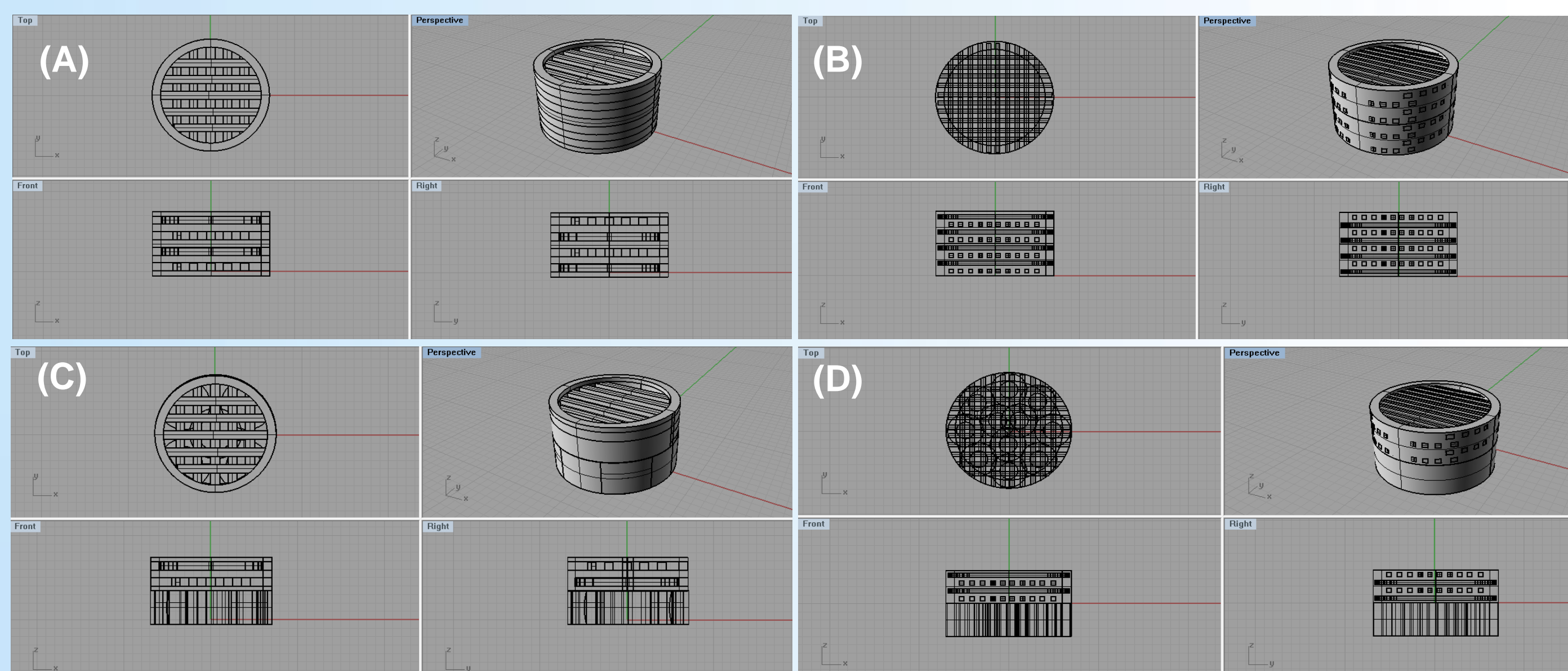


Figure 2. 3D printing models of osteochondral constructs with (A) & (B) homogeneous cross-hatched design with large and small pore features; (C) & (D) bi-phasic design with large and small pore features.

Results

3D printing osteochondral scaffold design (II)

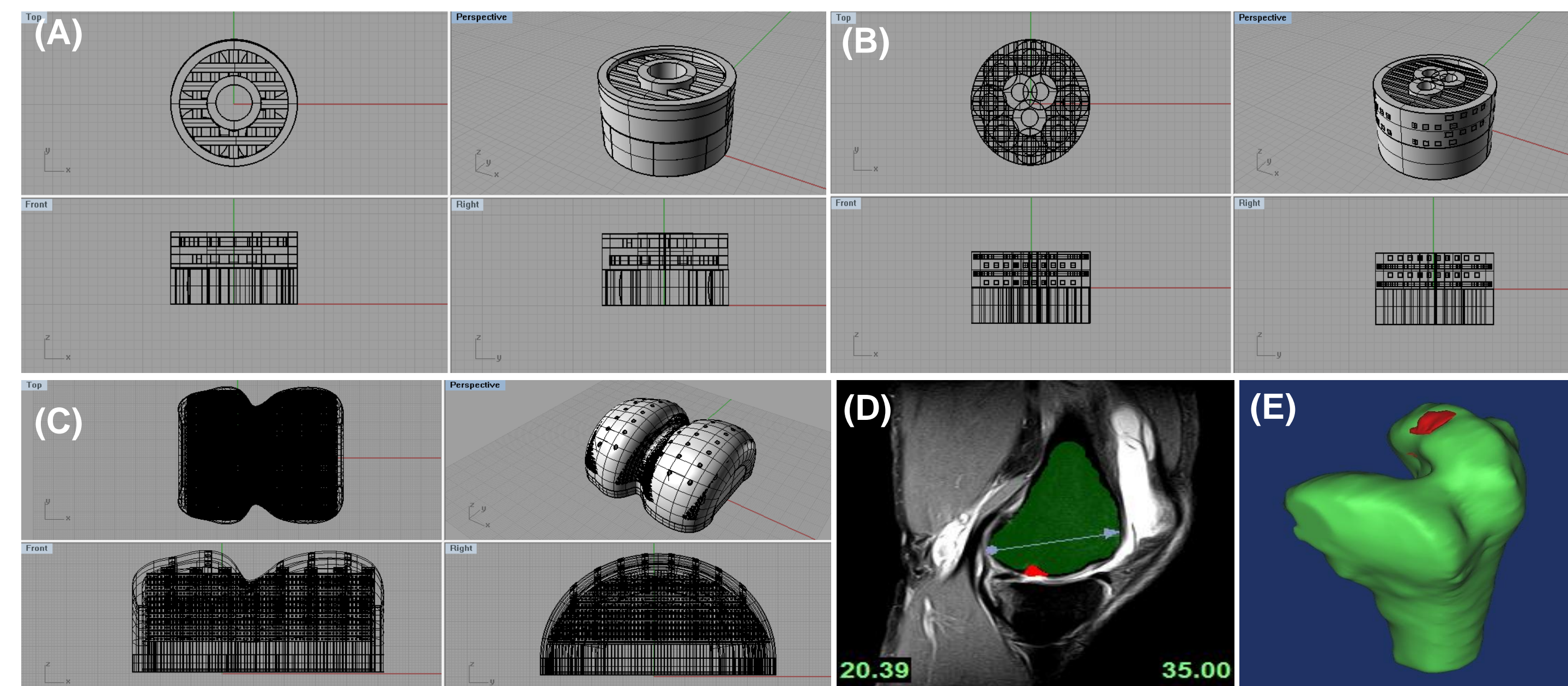


Figure 3. 3D printing models of osteochondral constructs with (A) & (B) "Key" bi-phasic design with large and small pore features, (C) a full knee construct design, (D) MRI image of the distal human femoral head (in green) with an articular osteochondral defect (in red) and (E) reverse-engineered 3D computational model.

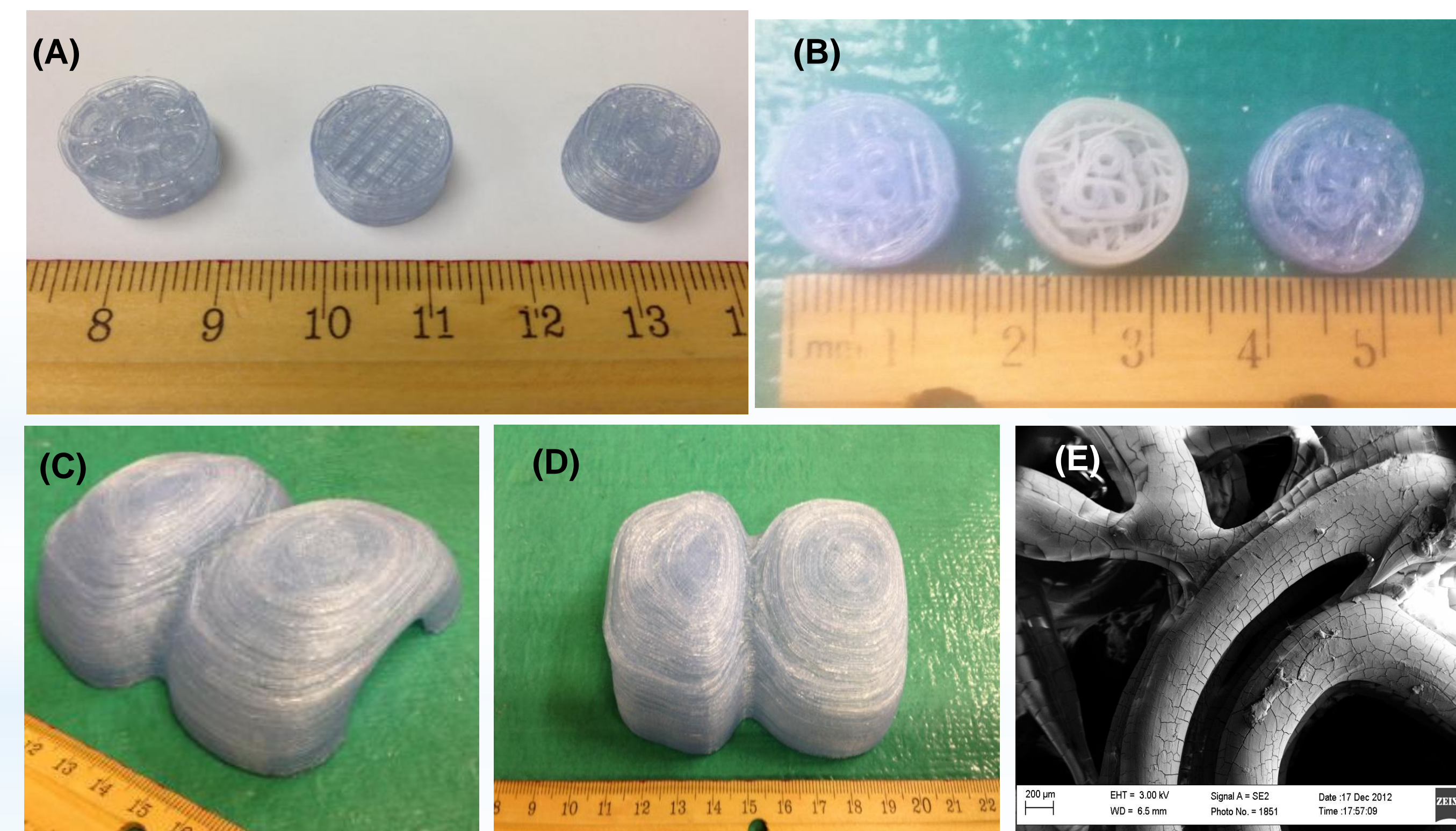


Figure 4. (A) Images of 3D printed bi-phasic, homogenous and bi-phasic (with a key feature) constructs in large pore features; (B) from left to right, a plain scaffold (bi-phasic with key and small pore features), a collagen coated scaffold and a MWCNTs poly-L-lysine coated scaffold; and (C)-(D) Images of fabricated full knee constructs (PLA) with anatomical shape. (E) Scanning electron microscopy image of a 3D printed collagen coated osteochondral scaffold.

Table 1: 3D printed scaffolds' physical characteristics

	Large pore feature			Small pore feature		
	Homogeneous	Bi-phasic	Bi-phasic Key	Homogeneous	Bi-phasic	Bi-phasic Key
Smallest Feature (mm)	1	1 ~ 4	1 ~ 4	0.5	0.5 ~ 2	0.5 ~ 2
Pore Density (pores/mm³)	0.5	0.2505	0.2505	5.3	2.6525	2.6526
Total Surface Area (mm²)	1850.644	2094.451	2150.739	2817.769	2854.017	2921.715
Total Volume (mm³)	616.379	716.219	749.803	571.185	863.646	947.439
SA/V Ratio	3.002	2.924	2.868	4.9331	3.305	3.084

Results

Mechanical characterization

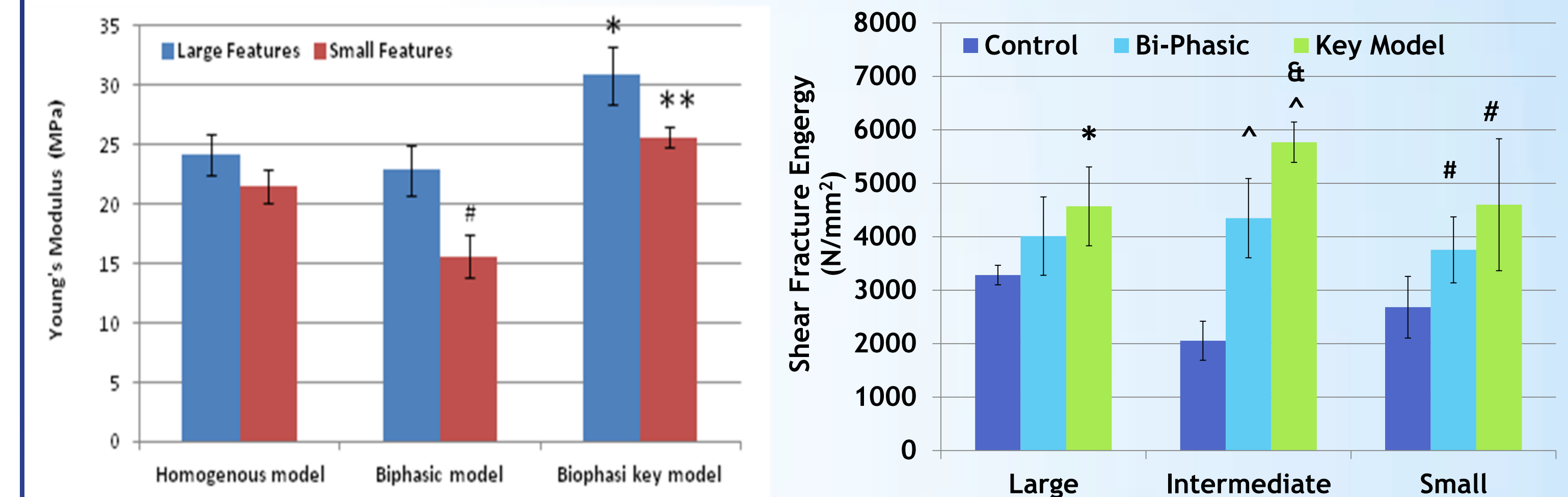


Figure 5: Compressive Young's modulus data for 3D printed scaffolds. Data are \pm SEM, n=5; *p<0.05 when compared to all homogenous and bi-phasic scaffolds; **p<0.05 when compared to all other scaffolds with small pore features; and #p<0.05 when compared to all other scaffolds.

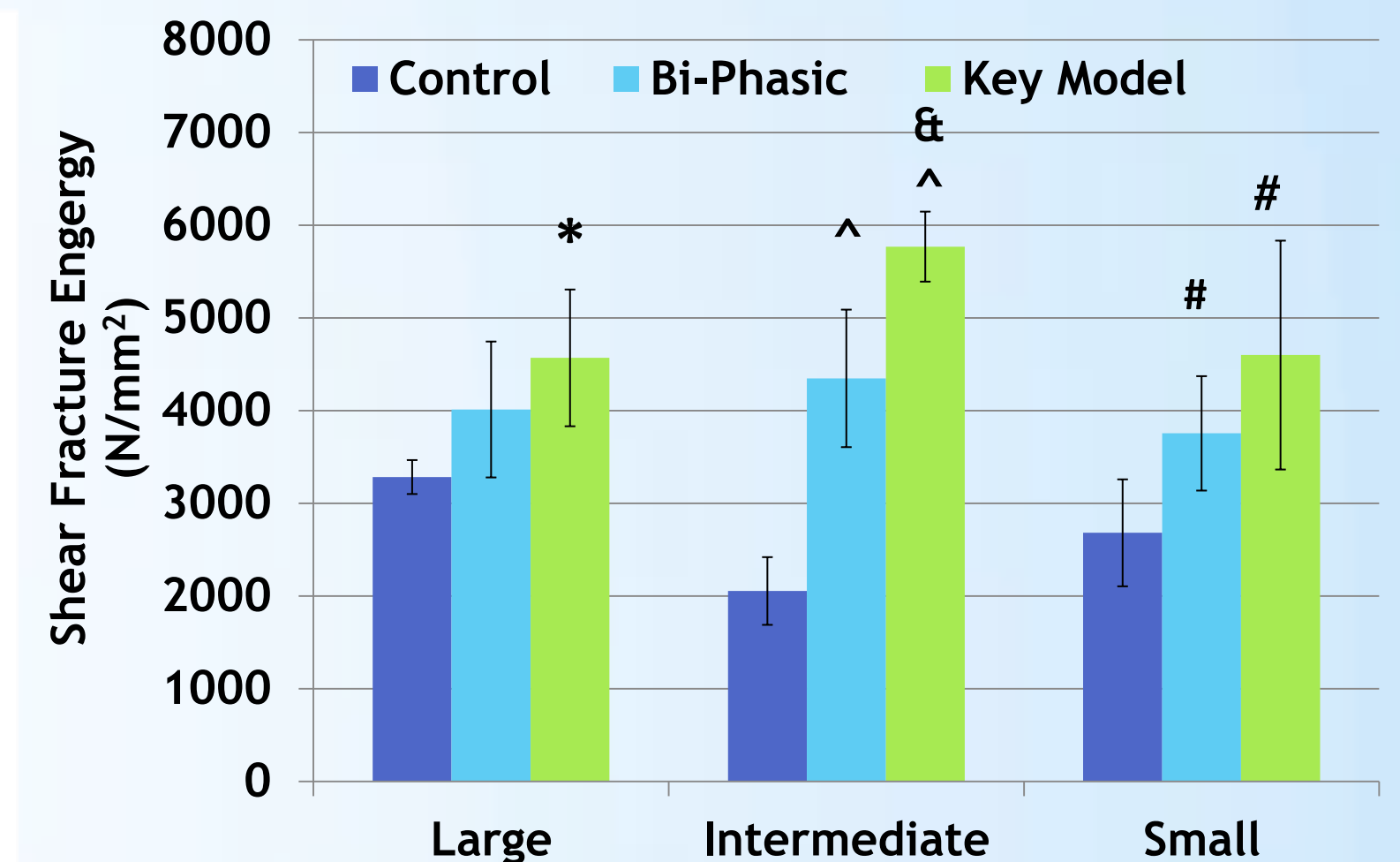


Figure 6: Shear fracture testing for 3D printed scaffolds. Data are \pm SEM, n=5; *p<0.1 when compared to controls at large pore feature; ^p<0.01 when compared to controls and &p<0.1 when compared to biphasic scaffolds with intermediate pores; and #p<0.1 when compared to controls with small pores.

Stem Cell Responses

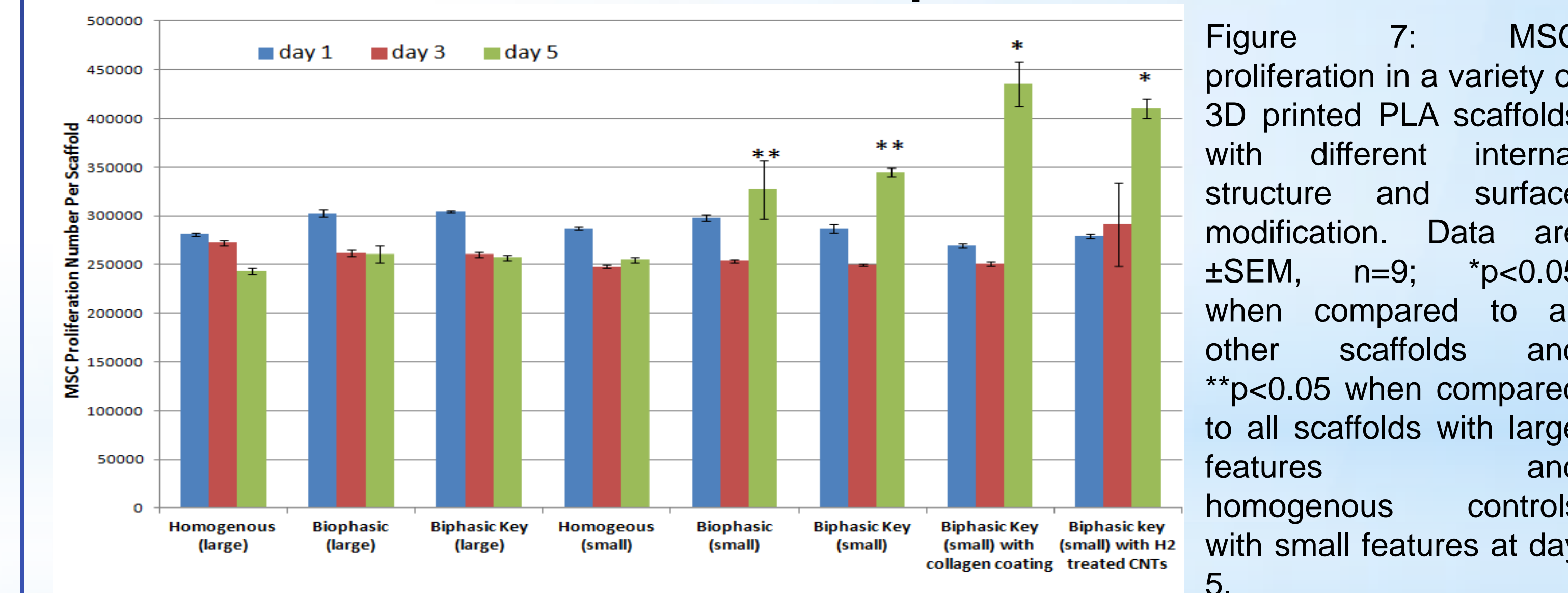


Figure 7: MSC proliferation in a variety of 3D printed PLA scaffolds with different internal structure and surface modification. Data are \pm SEM, n=9; *p<0.05 when compared to all other scaffolds and **p<0.05 when compared to all scaffolds with large features and homogenous controls with small features at day 5.

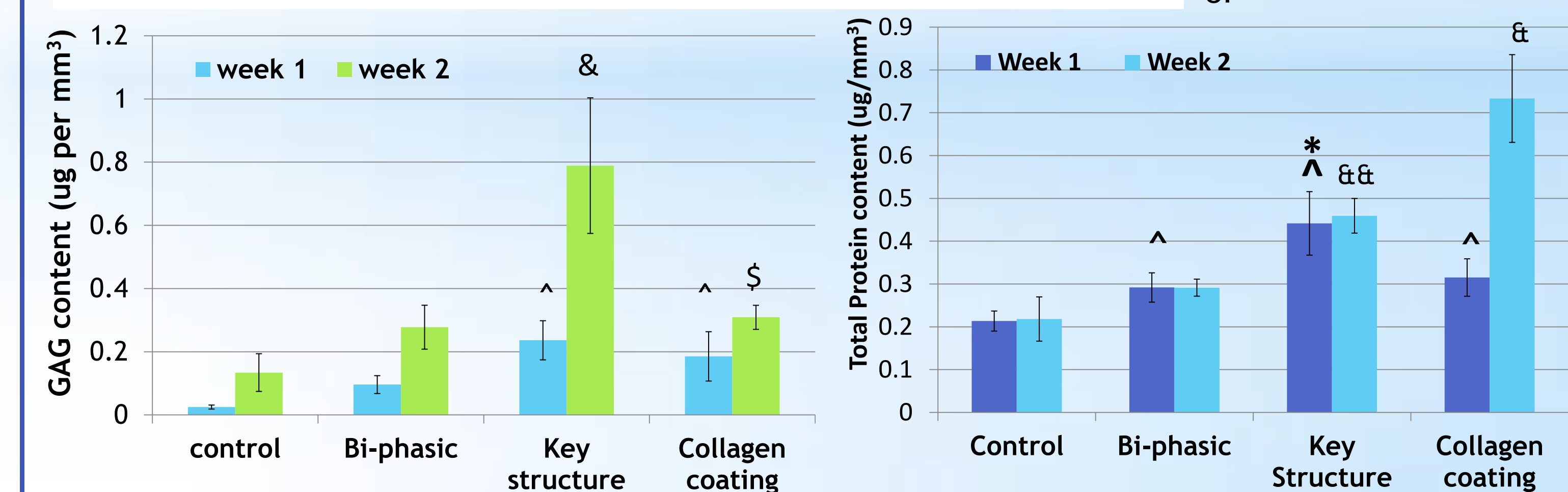


Figure 8: Glycosaminoglycan (GAG) synthesis in various 3D printed osteochondral scaffolds. Data are \pm SEM, n=9; &p<0.05 when compared to all other scaffolds and \$p<0.05 when compared to controls after two weeks; and ^p<0.05 when compared to controls and bi-phasic scaffolds after 1 week.

Figure 9: Total protein synthesis. Data are \pm SEM, n=9; ^p<0.05 when compared to controls and *p<0.1 compared to biphasic and collagen coated scaffolds after one week, &p<0.05 when compared to all other scaffolds and &&p<0.05 when compared to bi-phasic and controls after two weeks.

Conclusion

We created a series of novel biomimetic and bi-phasic osteochondral constructs that had excellent mechanical properties, cytocompatibility and anatomical shape for osteochondral tissue engineering applications. This study demonstrated that the design of both a bi-phasic construct and that of a mechanically enhanced key structure increased cellular activity, GAG synthesis, total protein deposition and the addition of an internal key feature enhanced the mechanical characteristics of the scaffold when compared to homogenous control scaffolds.

Acknowledgements

The authors would like to thank the Clinical and Translational Science Institute at Children's National (CTSI-CN) for financial support.